

# **EUROFEL-Report-2007-DS5-068**

## *EUROPEAN FEL Design Study*



Deliverable N°: D 5.2

Deliverable Title: Operational experience with the ELBE Superconducting RF photoinjector at high current

Task: DS-5

Authors: see next page

Contract N°: 011935

**Project funded by the European Community  
under the “Structuring the European Research Area” Specific Programme  
Research Infrastructures action**

## **EUROFEL Report**

### **Operational experience with the ELBE Superconducting RF photoinjector at high current**

Deliverable N°: D5.2

Deliverable Title: Operational experience with the ELBE Superconducting  
RF photoinjector at high current

Subtask : Superconducting RF Guns

Corresponding author: Jochen Teichert,  
Authors: A. Arnold, A. Büchner, H. Büttig, T. Kamps,  
F. Staufenbiel, R. Schurig, J. Teichert

Contract N°: 011935

## 1. INTRODUCTION

At the Forschungszentrum Dresden-Rossendorf (FZD) a superconducting radiofrequency photoelectron injector (SRF gun) has been designed, constructed and installed for operation at the electron accelerator ELBE. In this new type of RF injector, the photocathode is placed inside a superconducting acceleration cavity instead of a normal conducting copper cavity. The main advantage of the superconducting cavity is its low RF power dissipation which easily allows continuous wave operation. Thus the SRF gun has the potential to produce high-brightness electron beam with low transverse emittance at high bunch charge, as well as high average current.

At ELBE the new SRF gun will reduce the pulse length and the transverse emittance for the standard FEL operation mode with 77 pC bunch charge and 13 MHz pulse repetition rate compared to the existing thermionic electron injector. Using the SRF gun a second operation mode is now planned at ELBE with a bunch charge of 1 nC and a repetition rate of 500 kHz. This offers new applications in neutron physics and materials research with positrons. Furthermore, the SRF gun together with an extensive beam diagnostic will be available as a test stand for long term studies and optimization. It is envisaged to characterize the gun and to study different emittance compensation methods at high bunch charges up to 2.5 nC which is essentially important for future application of the SRF gun at the BESSY FEL. An overview of the gun parameters and planned operation modes is given in Table 1.

Table 1: Gun design parameters and expected beam values for the planned operation modes

	<b>ELBE mode</b>	<b>high charge mode</b>	<b>BESSY-FEL</b>
RF frequency	1.3 GHz		
beam energy	9.5 MeV		
Operation	CW		
drive laser wave length	262 nm		
Photocathode	Cs <sub>2</sub> Te		
quantum efficiency	>1 %		>2.5 %
average current	1 mA	0.5 mA	2.5 $\mu$ A
pulse length	5 ps	15 ps	40 ps
Repetition rate	13 MHz	500 kHz	1 kHz
bunch charge	77 pC	1 nC	2.5 nC
transverse emittance	1 $\mu$ m	2.5 $\mu$ m	3 $\mu$ m <sup>*)</sup>

<sup>\*)</sup> flat top laser

## 2. INSTALLATION AND COMMISSIONING

The main components of the SRF gun are the cryostat with the niobium cavity, the liquid helium supply line, the UV laser with the optical beam line, the rf system consisting of a klystron power source and the low-level control system, the equipment for the photocathode exchange, and the photocathode preparation laboratory. A 3D design picture of the SRF gun cryostat is presented in Fig. 1. Details of the SRF gun design are published in the paper of A. Arnold et al. [1].

After the final test of the niobium cavity in the vertical test bench and the He tank welding, the assembly of the cryostat started in spring 2007. During the summer shutdown of ELBE in June and July 2007, the cryomodule and the first part of the beam line were installed in the accelerator hall as it is shown in Fig. 2. The cryostat was connected to the He supply line of the ELBE refrigerator and the first cool-down was performed at the beginning of August 2007. In the following weeks the RF system was put into operation. Tests and measurements with low-power and later with high-power RF were carried out. At the same time the 500 kHz UV laser system was delivered and tested by MBI, and the optical components of the laser beam line were installed and adjusted.

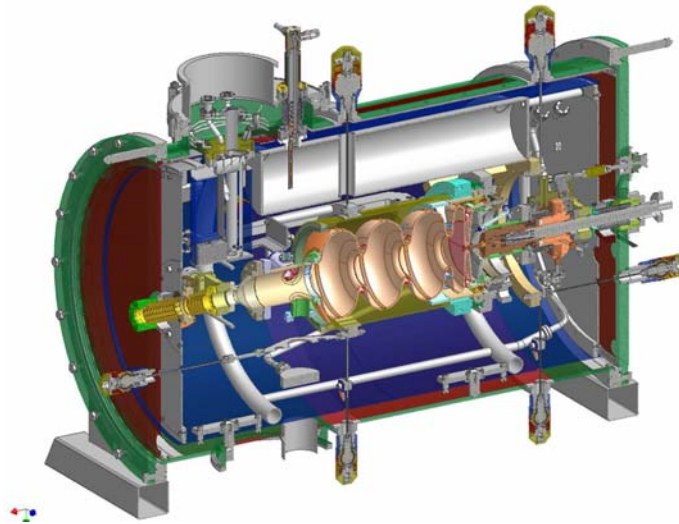


**Fig. 1: 3D cross section of the SRF gun cryostat.**

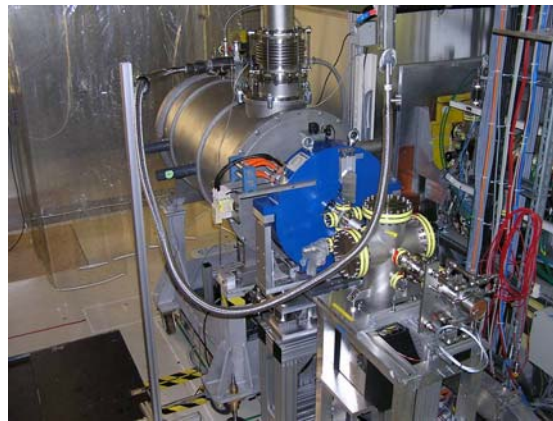


**Fig. 2: The SRF gun installed in the accelerator hall with emittance compensation solenoid and laser input port.**

The autumn shut-down of ELBE, in October 2007, was used to complete the installation of the diagnostics beam line. Designed and constructed by BESSY, this beam line is needed for the test, characterization and optimization of the SRF gun. Beside an emittance compensation solenoid downstream the gun and the beam optical components like quadrupoles and steerers, the beamline contains a diversity of diagnostics units as shown in Fig. 3. A Faraday cup, integrated current transformers (ICT) and beam dumps allow beam current measurements. Energy and energy spread can be determined by means of a C bend magnet. The transverse emittance of the beam can be measured with a slit mask system (EMS) and for the determination of bunch length two methods will be applied: Cherenkov radiation measurement with the streak camera and electro-optical sampling.

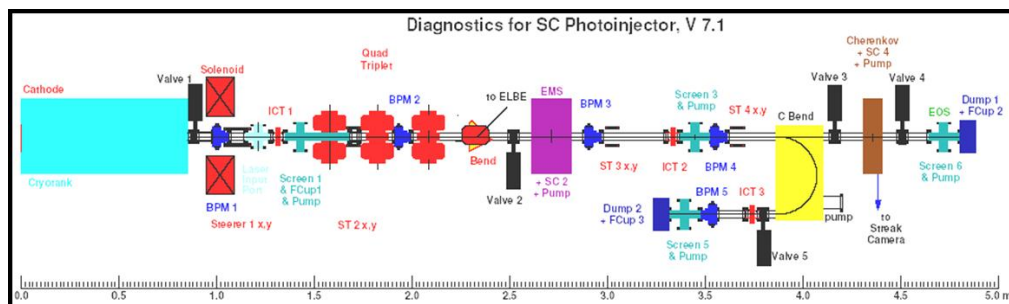


**Fig. 3: Diagnostics beamline installed at the SRF gun.**

End of October, the gun was cooled down for the second time. After readjustment of the laser beamline, putting into operation the power RF, the vacuum system, screen stations and some other components of the diagnostics beamline, the first electron beam could be produced on November 12, 2007.

Until end of 2007 the beam time was used for commissioning and test of further diagnostic components in the beam line and for a first characterization of the electron beam. Typical parameters are:

Laser: 0.4 W power @ 263 nm  
100 kHz pulse repetition rate  
4  $\mu$ J pulse energy  
15 ps (FWHM) pulse length (Gaussian)  
Photocathode: copper  
Quantum efficiency Q.E.  $\approx 10^{-6}$   
RF:  $f = 1300.38327$  MHz, 150 Hz bandwidth  
 $E_{\text{acc}} = 5$  MV/m,  $E_{\text{peak}} = 14$  MV/m  
rf power loss  $P_{\text{diss}} = 6$  W  
Electron beam: cw operation  
50 nA average current  
0.5 pC pulse charge  
2.2 MeV electron energy

During the winter shutdown in January 2008, the cathode transfer system will be installed. Then the copper photocathode can be replaced by Cs<sub>2</sub>Te photo cathodes allowing operation with higher bunch charges.

### **3. RF MEASUREMENTS**

#### **3.1 Summary of the measurements in the vertical test bench**

Between June 2006 and February 2007 four low temperature measurements of the cavity were carried out. For these measurements the cavity was prepared by buffered chemical polishing (40 $\mu$ m BCP) and high pressure rinsing (HPR). Afterwards the cavity was tested in the vertical cryostat at DESY. The results of these Q versus E measurements are shown in Fig. 4. Due to technical problems during the cleaning the achieved results of the followed 2<sup>nd</sup> and 3<sup>rd</sup> tests are unsatisfactory. Based on the experience of the first vertical test bench, an improved cleaning was realized by the company ACCEL Instruments. A special high pressure rinsing lance was built to enable an additional cleaning of the choke filter beside the established preparation of the cavity cells. Caused by the shortage of time the 4<sup>th</sup> preparation and the vertical test had to be the base for further assembly. The low performance is probably caused by field emitters due to insufficient cleaning and by a small scratch that we found inside the cavity at the back plane of the half cell. This damage results from a collision between the cavity and the high pressure rinsing lance during the cleaning. Even though the cavity performance keeps at a level of about 50% of the designed values, it will be possible to demonstrate the advantages and to collect important experiences in operation of such electron sources.

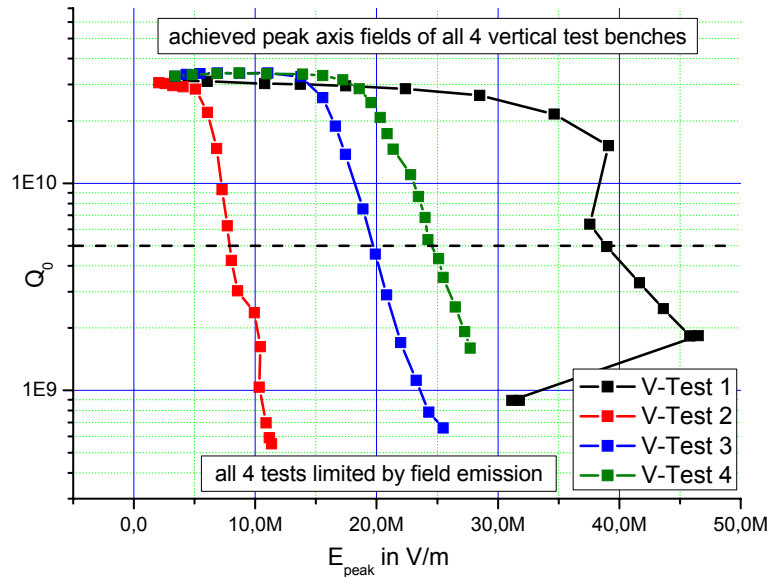


Fig. 4: Results of the cavity performance measurements at 1.8 K in the vertical test cryostat.

### 3.2 Cool-down to 2 K of the Gun Cryostat

The cool-down of the SRF gun in the ELBE accelerator hall started with the evacuation of the three volumes: isolation vacuum, beam line vacuum, and He tank vacuum. The influence on the cavity frequency is shown in Fig. 5.

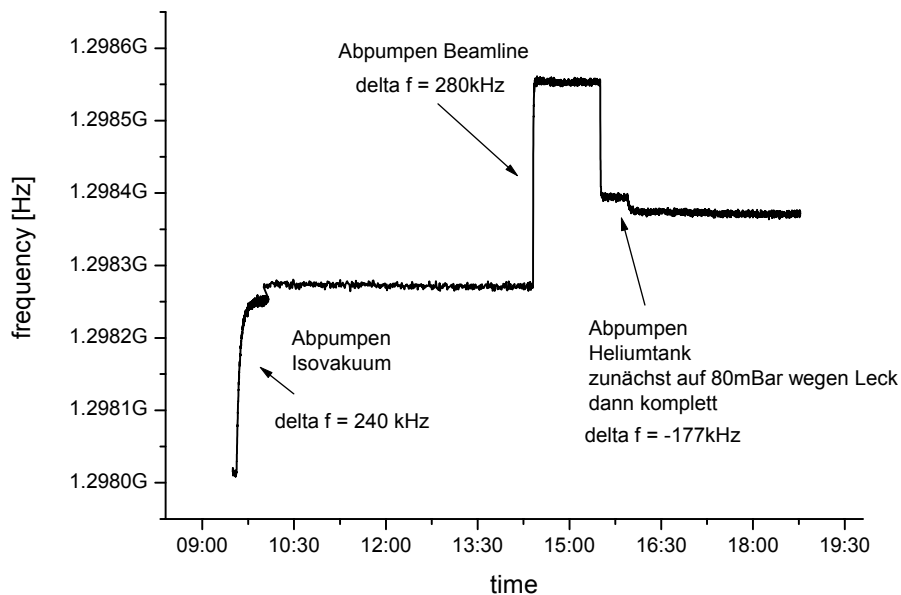
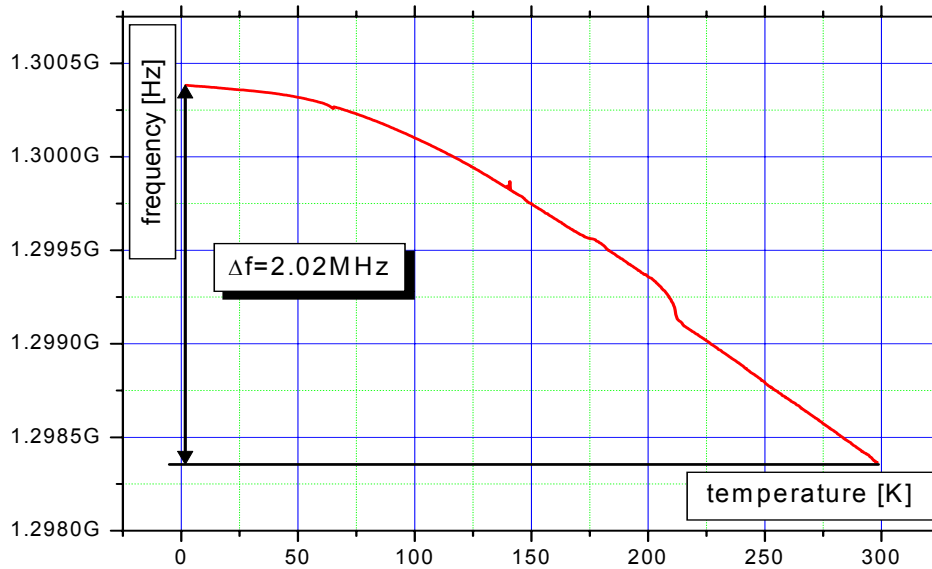


Fig. 5: Cavity frequency changes during pumping of isolation vacuum, beamline vacuum, and He tank vacuum.

Two days were used for cooling and filling of the liquid nitrogen tank for the thermal shield and the cathode cooler. After that the temperature of the cavity was still about 200 K. Then the cavity was cooled down with 10 K helium gas for about 24 h. After a break in which the two ELBE modules were cooled with helium gas the helium tank was filled with liquid He. Finally, the tank was pumped to 30 mbar in order to get the working temperature of 2 K.

Pressure stabilization is performed with cold compressors for all three cryostats (ELBE 1, ELBE 2, SRF gun) together using a pressure sensor near the ELBE 1 cryomodule. The frequency of the SRF gun cavity during the cool-down is plotted in Fig. 6. For the frequency shift from RT to 2 K a value of 2.02 MHz was found which is equal to the frequency shift of TESLA resonators in the ELBE cryomodules. Unfortunately, the pre-stress of the SRF gun tuners were wrong. Thus the final frequency which has been obtained is about 400 kHz too high.



**Fig. 6: Temperature dependence of the SRF gun cavity frequency measured during the cool-down in August 2007.**

### 3.3 Cavity performance measurement

The SRF gun cryostat has an electrical heater in the helium tank. For regular operating conditions, the liquid He flow into the cryostat is constant. The different consumption due to variations of the acceleration gradient is compensated by adequate changes of the heater power. It is controlled by a level sensor in the He tank. Therefore the change of the heater power between switched-off RF and a given gradient is equal to the RF loss of the cavity. These values were measured as function of the acceleration gradient. For the Q versus E the results in Fig. 7 are obtained. The red curve in the figure shows the corresponding radiation level due to the field emission in the cavity. It is obvious that the drop down of  $Q_0$  is connected to the field emission.

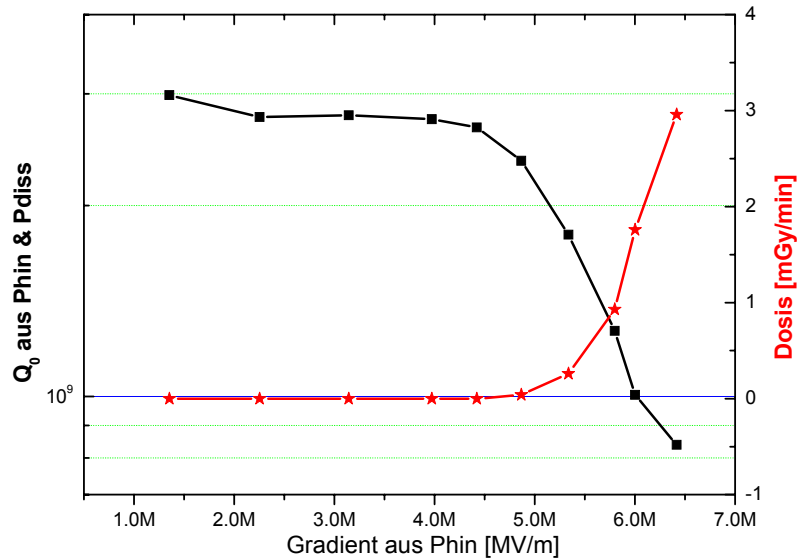


Fig. 7: Quality factor  $Q_0$  versus acceleration gradient and corresponding field emission dose.

### 3.4 Pressure Sensitivity

In order to estimate the pressure sensitivity of the cavity, the resonant frequency and the pressure of the helium liquefier were measured at the same time for 12 hours. The result is shown in Fig. 8. Apparently, there are frequency peaks that are not correlated with the pressure in helium system but they occur at the same time when the liquid nitrogen shielding is filled. We guess that the amount of gaseous nitrogen during the first time of the filling process is increasing the pressure in the feed pipe of the shielding, which probably results in detuning effect on the cavity. For the first test operation this is not a limiting fact, because the filling cycle is in the order of 3-4 hours. To eliminate this influence some design modifications will be implemented during the next warm up and modification phase in the third quarter next year.

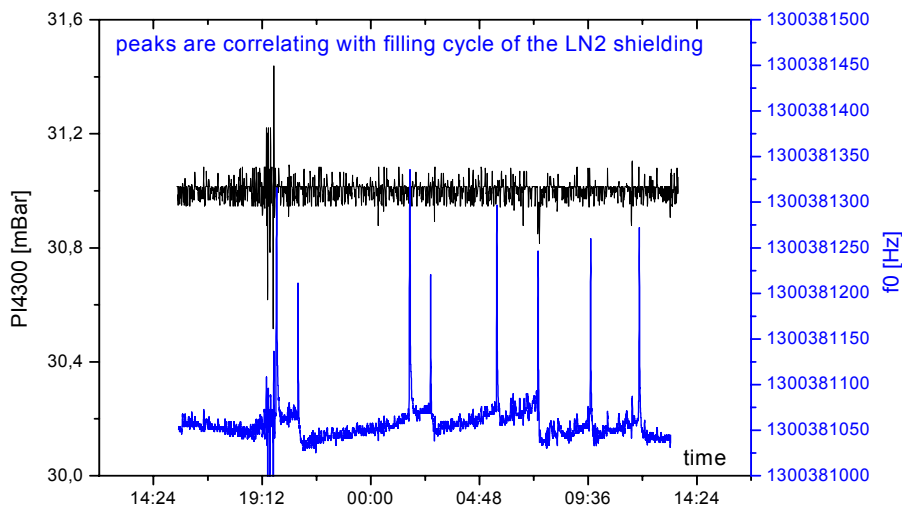


Fig. 9: Time domain plot of the resonant frequency and the helium pressure.

In order to get the pressure dependence of the resonant frequency, some minutes of the time domain frequency signal are plotted versus the pressure variation at the same time. The following linear fit function gives us a slew rate of approximately  $SR=230$  Hz/mbar (cp. Fig. 9).

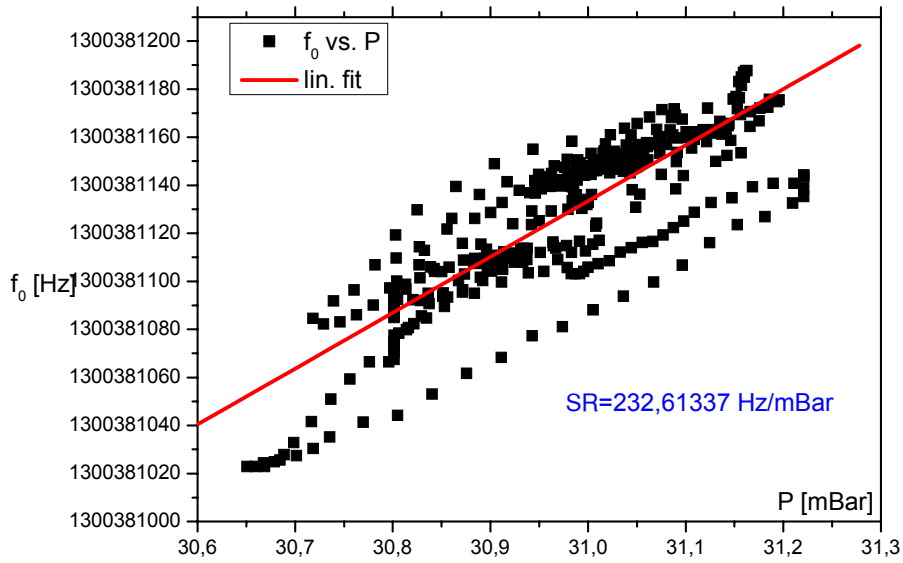


Fig. 9:  $f_0$  vs. helium pressure with fitted straight line.

In comparison to the measured value of  $SR=35\text{Hz/mbar}$  for the ELBE modules, the value is eight times higher. This could be a problem for operations at a high level of dissipated power which causes slow oscillations of the helium pressure ( $f > 1$  min) and thus the phase controller could exceed its regulation limit.

Beside additional design modifications of the cavity itself, also a control loop using the phase signal and the forward power as process variable and the cavity tuner as actuator could be used to improve the frequency behaviour.

### 3.5 Lorentz Force Detuning

In order to measure the Lorentz force detuning of the SRF-Gun cavity, a network analyzer (NWA) was used as a driver unit for the klystron amplifier. Due to the fact that an increasing RF field is detuning the frequency downward, the NWA has to sweep the klystron from higher frequencies over the cavity resonance to lower values. Otherwise the maximum field could not be reached. To increase the cavity field, the output power of the NWA was raised in steps of 1dB while the gradient was calculated by the calibrated pickup voltage. The achieved typical transmission plots are shown in Fig. 10.

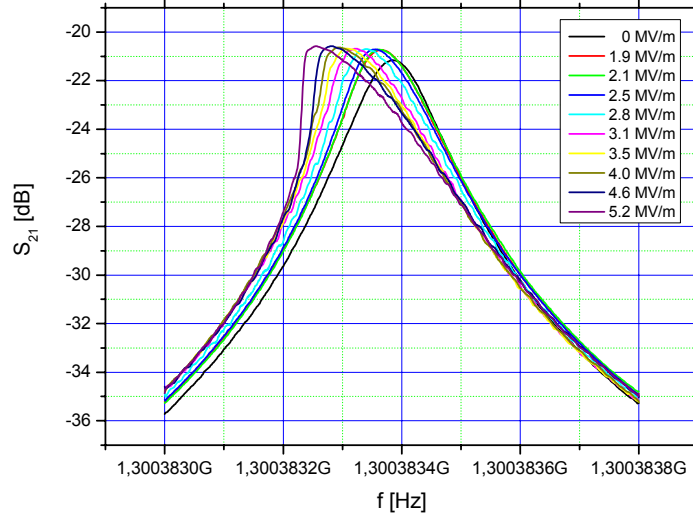


**Fig. 10: Measurement of the transmitted signal  $S_{21}$  for increasing gradients.**

If the frequency shift on crest is plotted versus the applied effective acceleration field in the cavity (cp. Fig. 11) one can find a quadratic dependence which can be explained by the radiation pressure that is proportional to quadratic field components

$$P_{rad} \propto \mu_0 H^2 - \epsilon_0 E^2 \quad (0.1)$$

and thereby the frequency shift is caused by deformation in a similar way (ref. 2).

$$\Delta f \propto (\epsilon_0 E^2 - \mu_0 H^2) \Delta V \quad (0.2)$$

The determined constant of proportionality can be found to be

$$\Delta f = a x^2 \quad ; \quad a_{gun} = -5 \text{ Hz} / (\text{MV} / \text{m})^2 \quad (0.3)$$

In comparison to the known value of the ELBE modules (ref. 3)

$$\Delta f = a x^2 \quad ; \quad a_{ELBE} = -0.9 \text{ Hz} / (\text{MV} / \text{m})^2 \quad (0.4)$$

the detuning of the SRF-Gun is five times higher. One cause could be the mechanical weak half cell. For practical operation at gradients of  $E_{acc} = 5\text{-}6 \text{ MV/m}$  the frequency shift is in the order of one bandwidth.

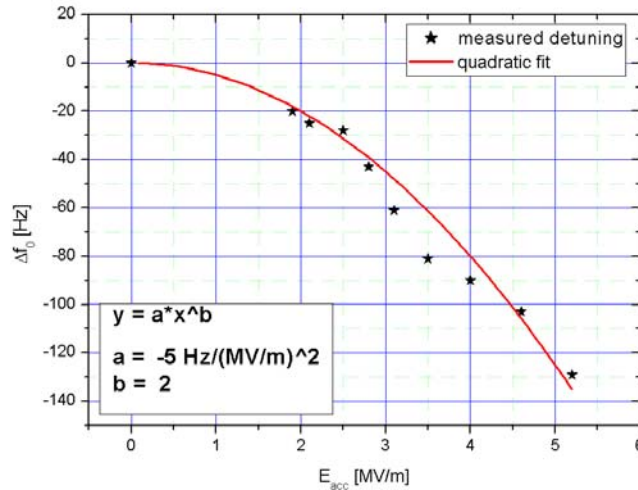


Fig. 11:  $\Delta f$  vs. gradient.

## 4. ELECTRON BEAM MEASUREMENTS

### 4. 1 Beam shape, current and bunch charge

The electron beam has been generated from a Cu photo cathode with a laser power of about 0.4 W at a repetition rate of 100 kHz and an acceleration gradient of 5 MV/m in the gun cavity. The beam could be imaged onto the YAG screens in the diagnostics beamline. Fig. 12 shows a typical picture with beam on screen 1 and the solenoid switched off. The size of the beam is about 11 mm x 2 mm (FWHM). On Fig. 13 the beam is focused on screen 1 with the emittance compensation solenoid (33 A).

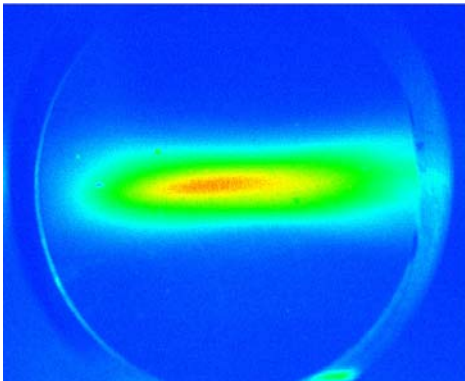


Fig. 12: Beam on screen 1, solenoid off.

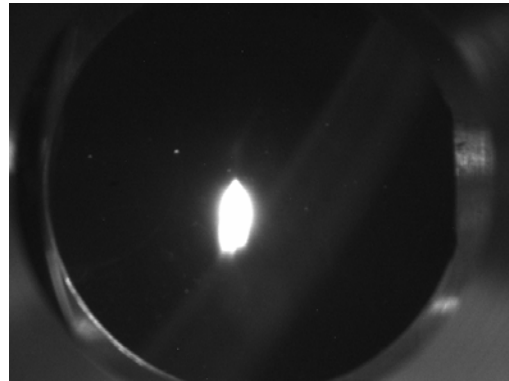


Fig. 13: Beam on screen 1, solenoid with  $I = 33A$ .

The electron beam was measured with a movable Faraday cup at the same beam line position as screen 1. The electron current was measured to about 50 nA at 0.4 W laser power. This value gives a bunch charge of 0.5 pC and a quantum efficiency of the photo cathode of about  $Q.E. = 10^{-6}$ .

### 4.2 Electron Energy

Electron energy measurements were carried out with the 180 degree dipole magnet (c bend) in the diagnostics beamline and imaging onto the following screen 5. Fig. 14 presents the electron energy versus the laser phase for a gradient of 5 MV/m.

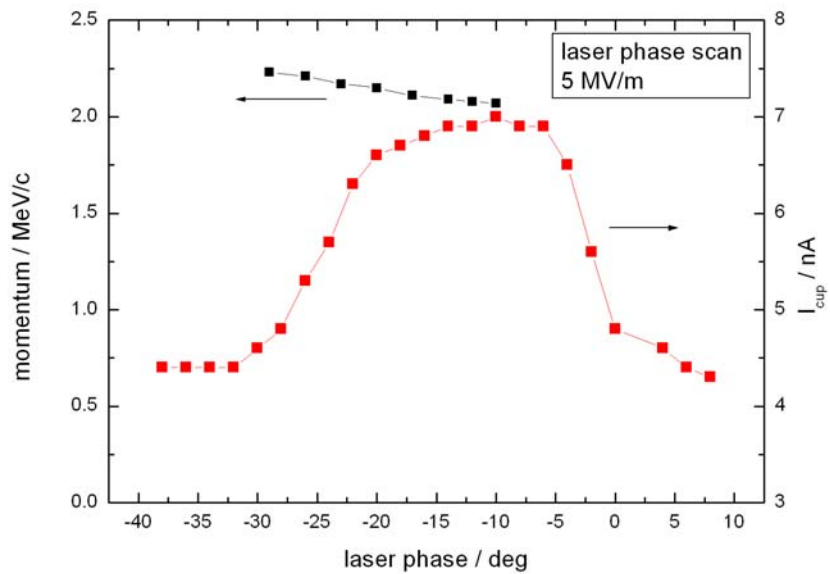


Fig. 14: Beam energy and Faraday cup current versus laser phase (0.03 pC bunch charge).

### 4.3 Phase Scan

A further laser phase (electron transmission) is shown in Fig. 15. This measurement is for a bunch charge of 0.3 pC. With solenoid the beam was focused into the Faraday cup. Up to now, the zero position of the laser phase is arbitrary.

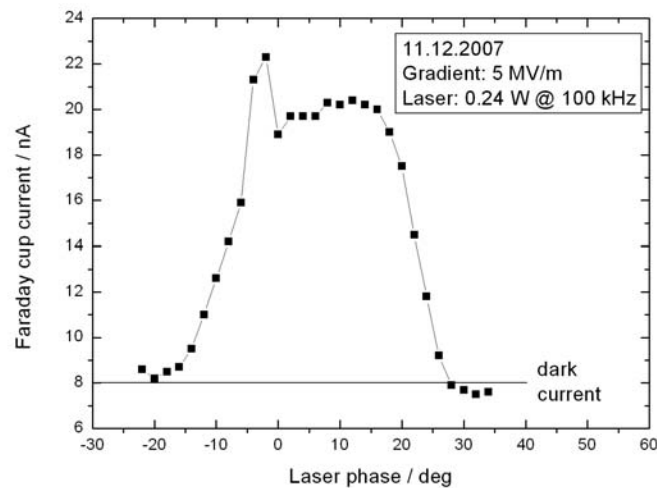
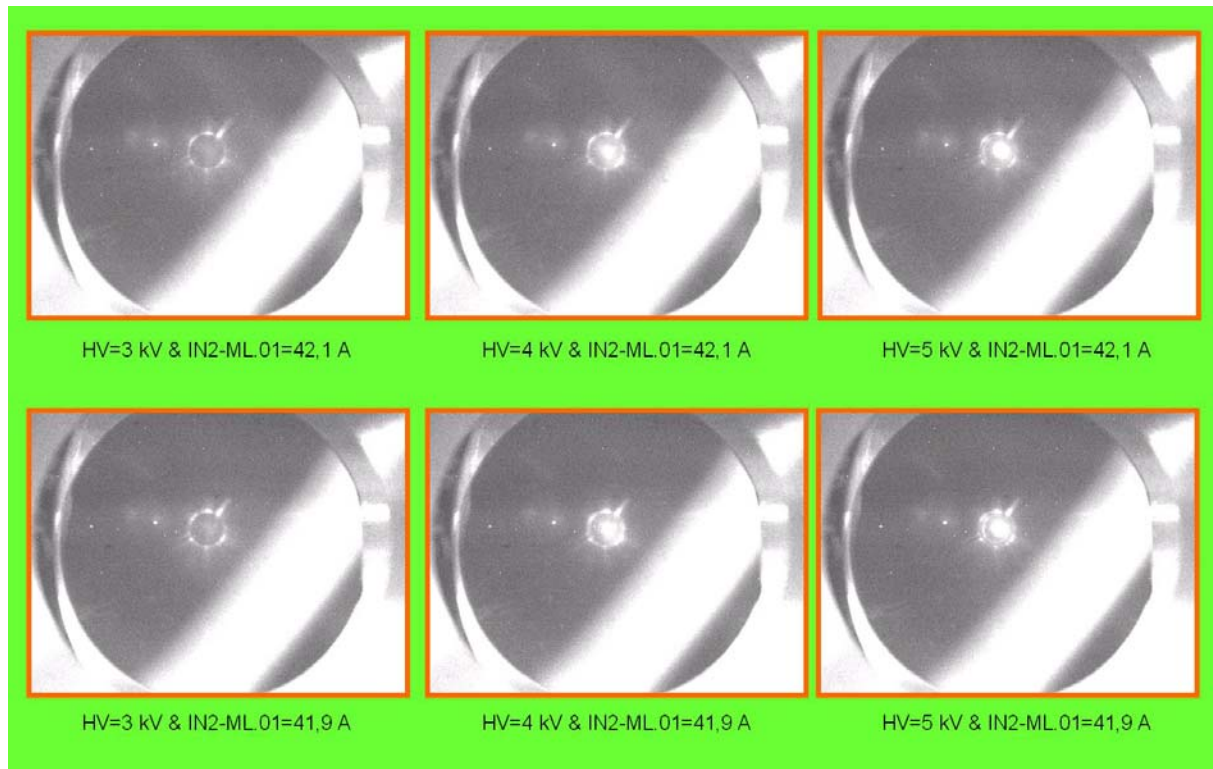


Fig. 15: Electron transmission versus laser phase.

### 4.4 Dark Current

The dark current which originates from the photocathode or its vicinity and has nearly the same energy as the beam was between 5 and 8 nA. The dark current could be measured in the Faraday cup and as emission current from the photo cathode itself. By means of the solenoid it was possible to obtain dark current images of the photo cathode as it is presented in Fig. 16. The images are for different focusing strength of the solenoid (41.1 A and 41.9 A) and

different DC voltage applied to the cathode. For higher DC voltage a bright spot appeared in the centre of the cathode. The reason for this effect is not clear up to now.



**Fig. 16: Dark current images of the cathode onto screen 1 using the solenoid.**

## 5. SUMMARY AND OUTLOOK

- The modified He supply system works well and no interferences with the ELBE cryomodules were observed. Thus parallel operation of ELBE and SRF-Gun is possible.
- The cavity performance is similar to that measured in the last vertical test. Only a low gradient ( $E_{acc} \leq 6$  MV/m,  $E_{peak} \leq 17$  MV/m) is available due to field emission. But the measured  $Q_0 = 3 \times 10^9$  is lower than that measured in the vertical test. It will be tried to reduce the field emission by means of in-situ RF processing or He processing.
- The cavity is more sensitive to He pressure fluctuation and has higher Lorentz force detuning than TESLA cavities.
- The 500 kHz UV Laser works fine. Laser diagnostics (virtual cathode), variable repetition rate and spot size variation have to be installed.
- The first electron beam with the Cu cathode could be produced. The gun allows stable and reproducible operation. Until end of 2007 the Cu cathode has been used to test all beam line components and diagnostics.

The problems which occurred during the cavity cleaning and the repeated measurements in vertical test stand required much more time than expected. Furthermore the three-shift operation of ELBE limits the access to the accelerator hall seriously. Installation work could only be carried out during the relatively short shut-downs every three months. For the next shut-down in January 2008, the installation of the cathode transfer system is scheduled.

The experimental work with the SRF gun will be continued in 2008. Especially the use of Cs<sub>2</sub>Te photocathode will then allow the study of such relevant problems like long term behavior and properties of photo cathodes at cryogenic temperatures as well as the cavity degradation topic. Further work will be concentrated to the emittance measurements and the emittance compensation methods suitable for SRF guns.

## REFERENCES

1. A. Arnold, et al., Development of a superconducting radio frequency photo injector, Nucl. Instr. and Meth. A577 (2007) 440.
2. Padamsee, H.; Knobloch, J., Hays, T.; Cornell University (Hrsg.): *RF Superconductivity for Accelerators*. New York, Ithaca: John Wiley & Sons INC, 1998. ISBN 0-471-15432-6
3. Andree Büchner, private communication